








RESEARCH ARTICLE | APRIL 12 2023

Bismuth trichloride as a molecular precursor for silicon doping

Eric A. S. Lundgren ; Rebecca Conybeare ; Taylor J. Z. Stock ; Neil J. Curson ; Oliver Warschkow ; Steven R. Schofield  



Appl. Phys. Lett. 122, 151601 (2023)

<https://doi.org/10.1063/5.0145772>



View
Online



Export
Citation

CrossMark

Articles You May Be Interested In

The origin of the conductivity maximum in molten salts. I. Bismuth chloride

J. Chem. Phys. (March 2012)

Optimization of thermoelectric properties in *n*-type SnSe doped with BiCl₃

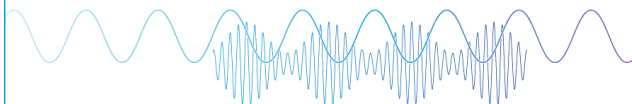
Appl. Phys. Lett. (February 2016)

Electrical Conductivity of Molten Bi–BiCl₃ and Bi–BiBr₃ Solutions

J. Chem. Phys. (May 2004)

Webinar

Boost Your Signal-to-Noise
Ratio with Lock-in Detection



Sep. 7th – Register now



Zurich
Instruments

Bismuth trichloride as a molecular precursor for silicon doping

Cite as: Appl. Phys. Lett. **122**, 151601 (2023); doi: [10.1063/5.0145772](https://doi.org/10.1063/5.0145772)

Submitted: 7 February 2023 · Accepted: 27 March 2023 ·

Published Online: 12 April 2023



View Online



Export Citation



CrossMark

Eric A. S. Lundgren,^{1,2}  Rebecca Conybeare,^{1,2}  Taylor J. Z. Stock,^{1,3}  Neil J. Curson,^{1,3} 
Oliver Warschkow,¹  and Steven R. Schofield^{1,2,a)} 

AFFILIATIONS

¹London Centre for Nanotechnology, University College London, London WC1H 0AH, United Kingdom

²Department of Physics and Astronomy, University College London, London WC1E 6BT, United Kingdom

³Department of Electronic and Electrical Engineering, University College London, London WC1E 7JE, United Kingdom

^{a)} Author to whom correspondence should be addressed: s.schofield@ucl.ac.uk

ABSTRACT

Dopant impurity species can be incorporated into the silicon (001) surface via the adsorption and dissociation of simple precursor molecules. Examples include phosphine (PH₃), arsine (AsH₃), and diborane (B₂H₆) for the incorporation of phosphorus, arsenic, and boron, respectively. Through exploitation of precursor surface chemistry, the spatial locations of these incorporated dopants can be controlled at the atomic scale via the patterning of a hydrogen lithographic resist layer using scanning tunneling microscopy (STM). There is strong interest in the spatial control of bismuth atoms incorporated into silicon for quantum technological applications; however, there is currently no known precursor for the incorporation of bismuth that is compatible with this STM-based lithographic method. Here, we explore the precursor chemistry (adsorption, diffusion, and dissociation) of bismuth trichloride (BiCl₃) on Si(001). We show atomic-resolution STM images of BiCl₃ exposed Si(001) surfaces at low coverage and combine this with density functional theory calculations to produce a model of the surface processes and the observed features. Our results show that, at room temperature, BiCl₃ completely dissociates to produce bismuth ad-atoms, ad-dimers, and surface-bound chlorine, and we explain how BiCl₃ is a strong candidate for a bismuth precursor compound compatible with lithographic patterning at the sub-nanometer scale.

© 2023 Author(s). All article content, except where otherwise noted, is licensed under a Creative Commons Attribution (CC BY) license (<http://creativecommons.org/licenses/by/4.0/>). <https://doi.org/10.1063/5.0145772>

Electronic devices that operate at the atomic scale can be fabricated in silicon using a scanning tunneling microscope (STM) as a tool to deterministically position individual phosphorus dopant atoms with nanometer precision;¹ recent examples include the single atom transistor² and a two qubit gate.³ Dopant positioning is achieved via the use of a hydrogen termination layer on the silicon (001) surface as a lithographic resist, patterned by STM, to spatially control the adsorption and dissociation of the phosphorus precursor compound phosphine (PH₃). Recent work has demonstrated that arsenic donors and boron acceptors can be deterministically positioned into silicon with nanometer precision in an analogous manner, using arsine (AsH₃)⁴ and diborane (B₂H₆)⁵ as the precursor species, respectively. Recently, the chloride compounds boron trichloride (BCl₃)^{6,7} and aluminum trichloride (AlCl₃)⁸ have been explored for acceptor positioning. Chlorine atoms, like hydrogen, are known to desorb from the silicon surface under thermal processing conditions and chlorine has been explored as an alternative resist layer.^{9,10}

Here, we present experiments reporting a precursor for spatially positioning bismuth into silicon using STM: bismuth trichloride (BiCl₃). Substitutional bismuth donors in silicon are of interest for quantum technological applications due to their deep electron binding energy,^{11,12} large hyperfine coupling, and a nuclear spin $I = 9/2$ that provide additional degrees of freedom for performing quantum logic operations.^{13–15} Using atomic-resolution STM imaging combined with density functional theory (DFT) geometry optimization and transition state calculations, we show that BiCl₃ adsorbs completely dissociatively on Si(001) to produce surface adsorbed chlorine and bismuth atoms, and thus, we find BiCl₃ to be a promising candidate for the controlled positioning of bismuth into silicon. That is, the dissociative adsorption of BiCl₃ into lithographically defined regions of clean Si(001) surface can be anticipated to produce single bismuth atoms in pre-defined locations in analogy to established processes for phosphine, arsine, and diborane.^{1,4,5}

We prepared Si(001) samples (arsenic-doped, 0.04–0.06 Ω cm) by degassing in ultrahigh vacuum ($< 2 \times 10^{-10}$ mbar) at 550 °C

overnight followed by flash annealing several times to 1150 °C for 10 s. BiCl_3 is relatively nontoxic solid that we have obtained in powder form (Fisher Scientific) and evaporated in a low temperature effusion cell (MBE Komponenten) held at 90 °C, with the silicon sample at room temperature. STM experiments were performed at room temperature in an Omicron GmbH LT-STM using chemically etched tungsten tips.

We have performed density functional theory (DFT) calculations using the hybrid exact-exchange functional B3LYP^{16,17} and the Gaussian 16 software.¹⁸ A $\text{Si}_{33}\text{H}_{28}$ cluster model was used to represent the Si(001) surface (see [supplementary material](#) Fig. 1). Twenty eight hydrogen atoms form a chemical termination for all silicon atoms other than the surface dimer atoms. These cluster-terminating hydrogen atoms were held in fixed positions during geometry optimization in order to emulate the strain that would be imposed by the surrounding surface and bulk atoms of an extended surface. Adsorption energies, E_{ads} , are calculated relative to the clean Si(001) surface and a gas phase BiCl_3 molecule. A detailed description of our computational methodology can be found in the [supplementary material](#) accompanying this Letter.

Figures 1(a) and 1(b) show filled- and empty-state images of a surface that has been exposed to BiCl_3 for one second with the sample at room temperature. The silicon dimer rows that run along the [110] direction are aligned running horizontally in the image. There are six key features in these images that can be attributed to the adsorption and dissociation of BiCl_3 . These features are highlighted by squares in Figs. 1(a) and 1(b), and enlarged in Figs. 1(c)–1(h), with corresponding structural schematics indicating our feature assignments. We did not identify any features other than these, and Figs. 1(a) and 1(b) are representative of the surfaces that we imaged following the exposure of Si(001) to BiCl_3 .

The three features labeled Cl1, Cl2, and Cl3 have been described previously in experiments in which the Si(001) surface was exposed to molecular chlorine (Cl_2) at room temperature.¹⁹ These features are composed of one or two chlorine atoms attached to the surface as shown in the accompanying schematics. Cl1 is two chlorine atoms adsorbed to a single dimer in a monochloride structure; Cl2 is two chlorine atoms bound to two neighboring dimers and leaving two dangling bonds at the ends of each dimer; and Cl3 is a single chlorine bound to a dimer, where there is also some motion of the chlorine atom from one end of the dimer to the other as the image is scanned, producing a streaky appearance for the features.¹⁹

In addition to these chlorine features, we see bright elongated features on the surface, labeled g1 and shown in Fig. 1(f). Such features have been previously observed in STM experiments of Si(001) surfaces exposed to low coverages of elemental bismuth via evaporation and are attributed to bismuth ad-dimers.^{20,21} Four configurations of bismuth ad-dimers are known to be stable from STM experiments and DFT calculations,^{22–24} where the ad-dimer bond is located either on top of the dimer row or in the trough between dimer rows, and the bond orientation is either parallel or perpendicular to the dimer row direction. In agreement with prior STM imaging²¹ and x-ray standing wave measurements,²⁵ we find the most common configuration is on top of the dimer rows with the ad-dimer bond parallel to the dimer rows, as shown in the schematic in Fig. 1(f).

The two other common features, labeled f1 and f2 in Figs. 1(g) and 1(h), have not been previously reported in the literature. Both features take the space of two surface dimers and have a single protrusion feature adjacent to a depression. For reasons that will be explained below, we assign these two features to a single bismuth ad-atom adjacent to two chlorine atoms adsorbed to the surface and they differ in the relative positioning of the chlorine and bismuth atoms: feature f1

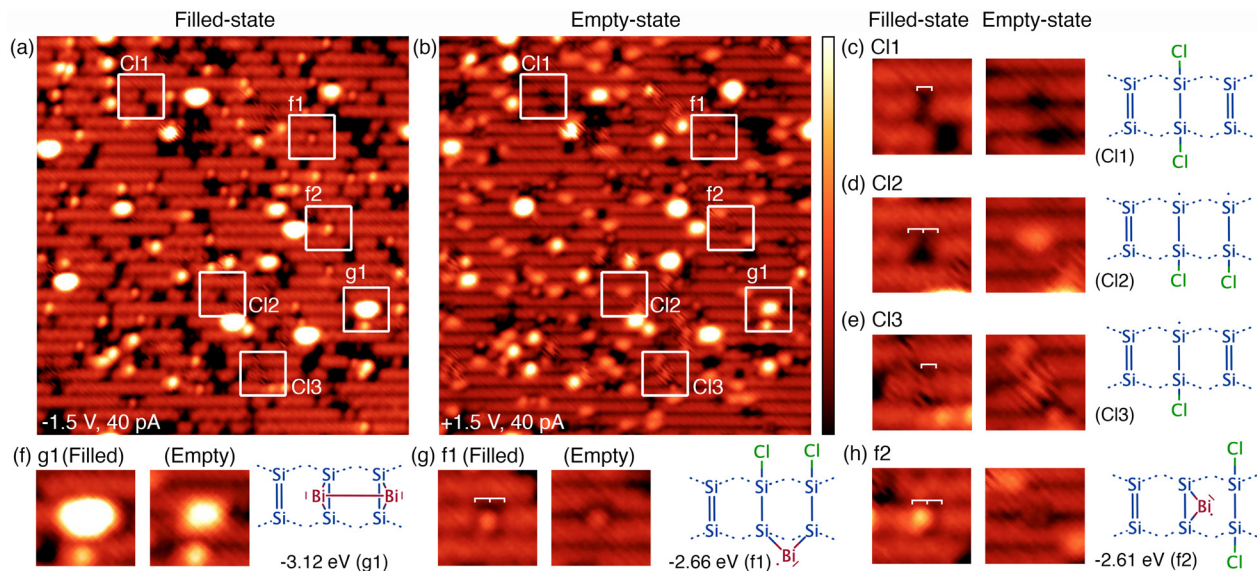


FIG. 1. (a) and (b) Filled- and empty-state images of a Si(001) surface exposed to a low coverage of BiCl_3 . Features attributable to BiCl_3 exposure are indicated by boxes and labeled Cl1, Cl2, Cl3, g1, f1, and f2 (Cl1, Cl2, and Cl3 correspond to chlorine adsorption features “type I,” “type II,” and “type III,” respectively, from Ref. 19). Enlarged versions of these features are shown in panels (c)–(h) with schematic diagrams indicating our structural assignments. Annotations on the STM images indicate the surface lattice constant separation. Image parameters (all images) ± 1.5 V, 40 pA, with z-range: 190 pm; (a)–(b) 23×23 nm² and (c)–(h) 2.7×2.3 nm².

has two chlorine atoms bonded to the ends of two silicon dimers, analogous to the Cl2 feature, and with a bismuth ad-atom bridge bonding across the two silicon atoms at the other ends of these dimers [Fig. 1(g)]; feature f2 has two chlorine atoms bound to a single dimer, analogous to the Cl1 feature, with a single bismuth ad-atom bridge bonding on the adjacent silicon dimer [Fig. 1(h)].

We have counted the total number of features of each type occurring in a set of images and the results are shown in Table I. The first column in the table shows the raw count of the number of times the feature was observed, and the following two columns convert the raw counts to numbers of bismuth and chlorine atoms, respectively, based on the feature assignments described above. We find the ratio of chlorine to bismuth atoms is 3.29:1, which is to within 10% of the expected 3:1 ratio of the BiCl₃ stoichiometry, providing additional observational support to our feature assignments.

To understand how and why these features form, we have performed DFT calculations to determine the geometry optimized thermodynamic minimum energy configurations and transition-state barrier energies relevant to the adsorption, diffusion, and dissociation of BiCl₃ on Si(001). The dissociation is driven by an increased thermodynamic stability as the adsorbates break apart on the surface, while the energetic barriers determine how fast the adsorbates diffuse or dissociate, and which routes are preferred. The energetics and key structures necessary to explain our experimental observations are presented below, and a full summary of our computational results can be found in the supplementary material.

Our experimental data show that many of the chlorine and bismuth atoms on the surface are spatially separated from one another. This suggests the diffusion of molecular fragments BiCl_x plays an important role in the dissociation pathway. With this in mind, it is instructive to first consider these BiCl_x fragments in isolation and establish their capacity for surface diffusion.

Similar to PH₃ and AsH₃, BiCl₃ has an electron lone pair that can readily form a dative bond with the electrophilic down-buckled atom of a silicon (001) surface dimer.²⁶ However, unlike PH₃ and AsH₃, we could not identify a configuration for molecularly adsorbed BiCl₃. Thus, our calculations suggest that the adsorption of BiCl₃ is dissociative and barrierless.

The BiCl₂ fragment forms a single Bi-Si bond at the end of a surface dimer in what we refer to as the *dimer-end* position [b3; -1.58 eV, Fig. 2(a)]. This structure can diffuse to an adjacent dimer via a

transition state, where BiCl₂ forms a second bond to the silicon atom of the neighboring dimer in the same row [Fig. 2(a)]. The calculated activation energy for this transition is $E_A = 0.55$ eV, which, combined with our calculated attempt frequency for this transition, produces a short mean lifetime (i.e., the time the adsorbate resides on one dimer) of 2×10^{-3} s (at 300 K), suggesting this diffusion is rapid at room temperature.

The thermodynamic minimum energy structure for an isolated BiCl fragment is in an *end-bridge* configuration, where BiCl forms two Bi-Si bonds to the ends of two adjacent silicon dimers [d4, -2.21 eV, Fig. 2(b)]. A slightly less stable configuration [e3; -2.20 eV, Fig. 2(b)], where BiCl is bridge-bound across a single surface dimer is separated by a transition state as shown in Fig. 2(b). Successive transitions between these configurations enable BiCl to diffuse along the dimer row with an overall activation barrier of 0.51 eV and mean lifetime of 8×10^{-5} s, implying rapid diffusion along the dimer row.

The dimer-bridge position [f7; -2.39 eV, Fig. 2(c)] is the preferred configuration for a bismuth ad-atom on the Si(001) surface. Bismuth ad-atom diffusion involves structure f9 [-2.01 eV, Fig. 2(c)], which is a closely related configuration, where the bismuth ad-atom forms a third bond to the adjacent dimer that we call the tripod structure. Diffusion of the bismuth ad-atom from one dimer to the next involves transitioning through two diagonally opposed tripod configurations, as illustrated in Fig. 2(c). The transition state separating these two structures is rate limiting with a barrier of 0.44 eV; correspondingly, the mean lifetime of a bismuth ad-atom with respect to diffusion is 4×10^{-4} s. The final step in the bismuth ad-atom diffusion is from structure f9 back to structure f7, but where the ad-atom is now bound to the next dimer along the dimer row.

The above results demonstrate that BiCl₂, BiCl, and bismuth ad-atoms all exhibit low barriers for diffusion along the dimer rows, consistent with our experimental observations of bismuth and chlorine spatially separated on the surface. To complete the explanation of the features we observed experimentally on the BiCl₃ exposed Si(001) surface, we have also calculated the barriers for dissociation to describe how the BiCl_x fragments break apart. A summary graph of the energetics is shown in Fig. 3(a). Also shown in this figure are the energies of the structures that we assign to the features observed in our experiments, namely, f1, f2, and g1, highlighted by solid circles. [The corresponding structural schematics were given in Figs. 1(f)–1(h).]

BiCl₂ [b3; -1.58 eV, Fig. 3(b)] can dissociate in two ways, by transferring the Cl atom either to the opposite end of the silicon dimer it is bound to (on-dimer dissociation) or to the silicon atom on the adjacent dimer (inter-dimer dissociation). On-dimer dissociation results in a more stable structure [c4, -1.91 eV, supplementary material Fig. 5(d)], but inter-dimer dissociation to structure c6 [-1.64 eV, Fig. 3(b)] is kinetically preferred due to lower activation energy (0.21 eV vs 0.35 eV). Furthermore, structure c6 readily stabilizes into structure d5 [-2.21 eV, Fig. 3(b)] that makes the dissociation reaction irreversible at room temperature. The lifetime of the BiCl₂ structure b3 with respect to dissociation is 3.2×10^{-9} s, which is too short-lived to be observable in our experiments, and is six orders of magnitude faster comparison to the diffusion of BiCl₂ discussed above.

BiCl can also dissociate to Bi + Cl, which proceeds via a two-step process where the end-bridge BiCl [d4, -2.21 eV, Fig. 3(c)] first converts to a dimer-bridge configuration [e3, -2.20 eV, Fig. 3(c)], resulting in a BiCl bridge-bonded to the two atoms of a single dimer.

TABLE I. Count of the number of each feature type within a set of STM images totaling a surface area of 5200 nm². The raw feature counts have also been converted into numbers of bismuth and chlorine atoms based on the assignments shown in Fig. 1. The total ratio of chlorine to bismuth is 3:1 to within an uncertainty of 10%.

Feature	Count	Bismuth	Chlorine
f1	78	78	156
f2	158	158	316
g1	148	296	0
Cl1	151	0	302
Cl2	446	0	892
Cl3	85	0	85
Total	1066	532	1751

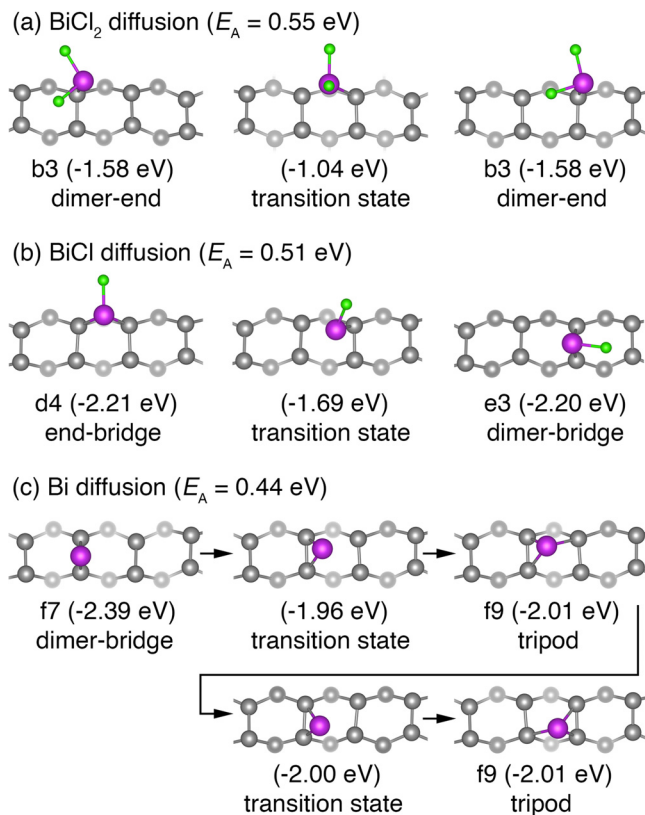


FIG. 2. Pathways for the dimer-row diffusion. (a) BiCl_2 diffusion takes place in a single step with BiCl_2 moving between the dimer-end position in two neighboring dimer via a transition state configuration where BiCl_2 forms bonds to both silicon atoms. (b) BiCl diffusion occurs in two stages with the BiCl moiety moving from the minimum energy end-bridge to a less stable dimer-end position. (c) Bismuth ad-atom diffusion occurs along the top of the dimer row with the bismuth atom moving between dimer-bridge and tripod configurations.

Once in the dimer-bridge configuration, the chlorine atom can dissociate to the dimer-end position of the adjacent silicon dimer, leaving a bismuth ad-atom in the dimer-bridge position to produce structure f4 [-2.45 eV, Fig. 3(c)]. This dissociated structure has gained 0.25 eV in stability relative to the BiCl configuration (d4). The rate limiting step for this dissociation of BiCl is the transition from the end-bridge to dimer-bridge configurations [d4–e3, shown in Fig. 2(b)], which is the same rate limiting step for BiCl diffusion. As such, the activation barriers for these two processes are the same [0.51 eV; Fig. 3(a)].

Thus, our calculations predict that BiCl_3 rapidly dissociates on $\text{Si}(001)$, in agreement with our experimental observations of a range of features attributable to bismuth and chlorine atoms attached to the surface. Furthermore, isolated bismuth atoms and BiCl fragments have diffusion lifetimes much faster than typical STM image acquisition timescales, explaining why these species are not observed. Next, we explain how the features observed in our experiments arise.

The two successive dissociation steps $\text{BiCl}_3 \rightarrow \text{BiCl}_2 + \text{Cl}$, and $\text{BiCl}_2 \rightarrow \text{BiCl} + \text{Cl}$ explain the observation of adsorbed chlorine atoms on the surface. Moreover, the barrier for BiCl_2 dissociation to BiCl is significantly smaller than the barrier for BiCl_2 diffusion,

suggesting that BiCl_2 dissociates in-place without diffusion of the BiCl_2 fragment. Together, these observations explain the occurrence of the Cl1 and Cl2 features, both of which consist of a pair of adjacent surface bound chlorine atoms.

The complete dissociation of the BiCl_3 fragment and the low barrier for bismuth ad-atom diffusion provide the opportunity for two bismuth ad-atoms to encounter one another and form a bismuth ad-dimer. We have calculated the barrier to the formation of an ad-dimer starting from two adjacent bismuth ad-atoms in the dimer-bridge and tripod configurations [f10; Fig. 3(d)]. The breaking of the third bond of the tripod structure and the formation of a bismuth-bismuth bond results in the bismuth ad-dimer, as shown in Fig. 3(d). This results in an overall energy barrier of 0.44 eV for the formation of a bismuth ad-dimer and an average lifetime of 4.9×10^{-6} s such that ad-dimers can be expected to readily form when two bismuth ad-atoms meet. The ad-dimer formation provides a significant increase in stability [g1, -3.12 eV, Fig. 3(d)] such that the reverse barrier is 1.43 eV and the process is irreversible at room temperature. As a result, the ad-dimers are stable and we observe these features in our STM images [Figs. 1(a), 1(b), and 1(f)].

We have shown that isolated bismuth ad-atoms diffuse much too readily to be observed in an STM experiment. However, when a diffusing bismuth ad-atom encounters a pair of chlorine atoms in the Cl1 or Cl2 configurations, structures f1 or f2 are formed with an energy gain of 0.27 and 0.22 eV, respectively, [Figs. 1(g), 1(h), and 3(a)]. These increases in stability increase the barriers to escape these conformations which contribute to making these features long-lived and therefore observable in our STM experiments. However, it stands to reason that the bismuth atoms from features f1 and f2 can diffuse away via the f7–f7 diffusion barrier and then pair up with other chlorine atoms or other bismuth atoms, to form new f1 or f2 features, or bismuth ad-dimers, respectively. Relative to f1 and f2 these barriers evaluate to 0.66 and 0.71 eV, which suggests that such processes would be apparent in our STM experiments. However, dynamical changes involving the f1 and f2 features have not been observed, implying that other higher barriers are involved in separating a bismuth atom from the f1 and f2 features.

Structure d1 [-2.63 eV; Fig. 3(a) and supplementary material Fig. S4(a)] is structurally similar to feature f1, with the modification that it has a BiCl , rather than a bismuth ad-atom, in the end-bridge location. The relatively strong thermodynamic stability of d1 and the relatively large barrier for its diffusion (1.04 eV assuming d4–d4 as rate limiting) suggest that it should be observable in STM images. However, our data are not consistent with the occurrence of both features f1 and d1. The absence of structure d1 in our experimental data can be attributed to the kinetic processes required for its formation. Calculation and comparison of the energetics and kinetics of all possible pathways is outside the scope of this manuscript. However, it is likely that it is the competition of diffusion and dissociation of BiCl that is the reason that d1 is not observed in experiment.

We have presented an investigation of the adsorption of bismuth trichloride on the silicon (001) surface. Using atomic-resolution STM measurements and DFT calculations, we have demonstrated that the adsorption is completely dissociative, resulting surface bound bismuth and chlorine atoms. These results are promising for the use of BiCl_3 as a precursor for the deterministic positioning of single bismuth atoms into silicon because (1) BiCl_3

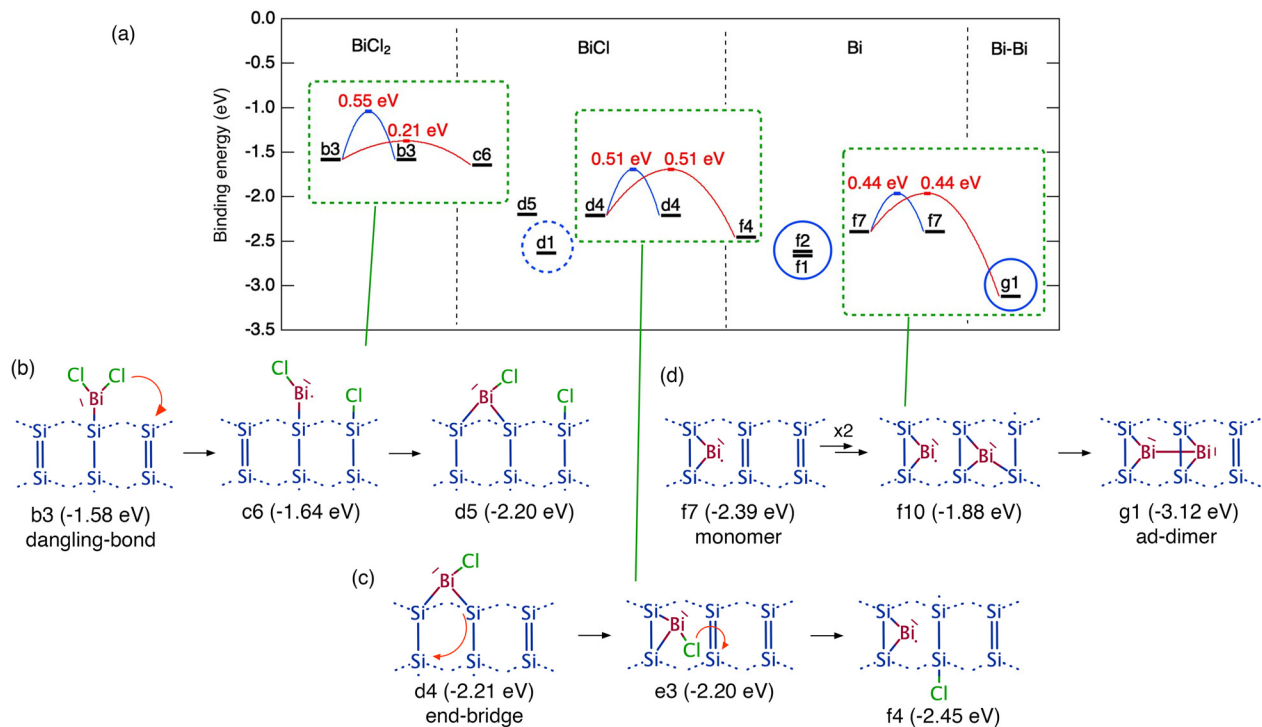


FIG. 3. (a) Calculated potential energies for key stages BiCl_3 dissociation on $\text{Si}(001)$, highlighting barriers for diffusion and dissociation of BiCl_2 and BiCl , as well as bismuth ad-atom diffusion and the formation of bismuth-bismuth ad-dimers. Schematic diagrams for the structures b3, c6, d4, d5, e3, f4, f7, f10, and g1 are shown in (b)–(d), which also highlight the key dissociation stages $\text{BiCl}_2 \rightarrow \text{BiCl} + \text{Cl}$ and $\text{BiCl} \rightarrow \text{Bi} + \text{Cl}$, and the formation of a bismuth-bismuth ad-dimer.

releases bismuth ad-atoms onto the $\text{Si}(001)$ surface on adsorption and (2) the only other species introduced to the surface are chlorine atoms that do not pose a fundamental limitation on device fabrication; i.e., it is known that chlorine can be desorbed from $\text{Si}(001)$ thermally,²⁷ or via direct stimulation using an STM tip.⁹ Moreover, it has been recently shown that chlorine atoms segregate to the surface during $\text{Si}(001)$ epitaxial growth, such that it may not be necessary to remove the chlorine at all.^{28,29} This desirable behavior for chlorine in regard to device fabrication can be contrasted to the behavior of carbon on $\text{Si}(001)$, which readily forms a silicon carbide upon annealing and requires extremely high temperatures to remove. This suggests that carbon-based precursor molecules are unlikely to find application for device fabrication.³⁰

Notwithstanding these strong benefits of BiCl_3 and chloride compounds in general for dopant precursors,^{6–8} there are several significant stages that remain to be demonstrated for atomically precise fabrication using BiCl_3 . Principal among these is the need to limit the formation of Bi-Bi ad-dimers. We suggest that this can be achieved through the use of an atomically precise resist to pattern areas of reactive silicon surface large enough to accommodate only one BiCl_3 adsorbate, e.g., a two- or three-dimer patch as is commonly used for atomically precise positioning of phosphorus dopants into silicon.^{1,2} This procedure would restrict bismuth atoms from diffusing and, therefore, inhibit Bi-Bi ad-dimer formation. The other key step that must be demonstrated is the substitutional incorporation of bismuth into the silicon surface. We anticipate this incorporation can be induced thermally by analogy to the behavior of the other group V

donors, P and As on both $\text{Si}(001)$ ^{1,4} and $\text{Ge}(001)$,^{31,32} and this is the focus of ongoing work in our laboratory.

See the [supplementary material](#) for a detailed description of our DFT computational methods and structure diagrams and calculated energetics for all structures considered in this work.

This project was supported by the EPSRC Project Atomically Deterministic Doping and Readout for Semiconductor Solotronics (No. EP/M009564/1). R.C. was supported by the EPSRC and SFI Centre for Doctoral Training in Advanced Characterisation of Materials (No. EP/L015277/1). T.J.Z.S. was partly supported by the JSPS/EPSC Core-to-Core Scheme under Project Defect Functionalized Sustainable Energy Materials: From Design to Device Application (No. EP/R034540/1). S.R.S. acknowledges the use of the UCL Myriad High Performance Computing Facility (Myriad@UCL).

AUTHOR DECLARATIONS

Conflict of Interest

The authors have no conflicts to disclose.

Author Contributions

Eric A. S. Lundgren: Data curation (lead); Formal analysis (equal); Writing – review & editing (equal). **Rebecca Conybeare:** Data

curation (equal); Formal analysis (equal); Writing – review & editing (equal). **Taylor J. Z. Stock:** Formal analysis (equal); Supervision (equal); Writing – review & editing (equal). **Neil J. Curson:** Formal analysis (equal); Supervision (equal); Writing – review & editing (equal). **Oliver Warschkow:** Formal analysis (equal); Supervision (equal); Writing – review & editing (equal). **Steven R. Schofield:** Conceptualization (lead); Formal analysis (lead); Supervision (equal); Writing – original draft (lead); Writing – review & editing (lead).

DATA AVAILABILITY

The data that support the findings of this study are available from the corresponding author upon reasonable request.

REFERENCES

- S. R. Schofield, N. J. Curson, M. Y. Simmons, F. J. Ruess, T. Hallam, L. Oberbeck, and R. G. Clark, "Atomically precise placement of single dopants in Si," *Phys. Rev. Lett.* **91**, 136104 (2003).
- M. Fuechsle, J. A. Miwa, S. Mahapatra, H. Ryu, S. Lee, O. Warschkow, L. C. L. Hollenberg, G. Klimeck, and M. Y. Simmons, "A single-atom transistor," *Nat. Nano* **7**, 242–246 (2012).
- Y. He, S. K. Gorman, D. Keith, L. Kranz, J. G. Keizer, and M. Y. Simmons, "A two-qubit gate between phosphorus donor electrons in silicon," *Nature* **571**, 371–375 (2019).
- T. J. Stock, O. Warschkow, P. C. Constantinou, J. Li, S. Fearn, E. Crane, E. V. Hofmann, A. Kölker, D. R. McKenzie, S. R. Schofield, and N. J. Curson, "Atomic-scale patterning of arsenic in silicon by scanning tunneling microscopy," *ACS Nano* **14**, 3316–3327 (2020).
- T. Škereň, S. A. Köster, B. Douhard, C. Fleischmann, and A. Fuhrer, "Bipolar device fabrication using a scanning tunnelling microscope," *Nat. Electron.* **3**, 524–530 (2020).
- K. J. Dwyer, S. Baek, A. Farzaneh, M. Dreyer, J. R. Williams, and R. E. Butera, "B-doped δ -layers and nanowires from area-selective deposition of BCl_3 on Si(100)," *ACS Appl. Mater. Interfaces* **13**, 41275–41286 (2021).
- T. V. Pavlova and K. N. Eltsov, "Reactivity of the Si(100)- 2×1 -Cl surface with respect to PH_3 , PCl_3 , and BCl_3 : Comparison with PH_3 on Si(100)- 2×1 -H," *J. Phys.: Condens. Matter* **33**, 384001 (2021).
- M. S. Radue, S. Baek, A. Farzaneh, K. J. Dwyer, Q. Campbell, A. D. Baczewski, E. Bussmann, G. T. Wang, Y. Mo, S. Misra, and R. E. Butera, "AlCl₃-dosed Si(100)- 2×1 : Adsorbates, chlorinated Al chains, and incorporated Al," *J. Phys. Chem. C* **125**, 11336–11347 (2021).
- K. J. Dwyer, M. Dreyer, and R. E. Butera, "STM-induced desorption and lithographic patterning of Cl-Si(100)- (2×1) ," *J. Phys. Chem. A* **123**, 10793–10803 (2019).
- E. Frederick, K. J. Dwyer, G. T. Wang, S. Misra, and R. E. Butera, "The stability of Cl-, Br-, and I-passivated Si(100)- (2×1) in ambient environments for atomically-precise pattern preservation," *J. Phys. Condens. Matter* **33**, 444001 (2021).
- A. L. Saraiva, A. Baena, M. J. Calderón, and B. Koiller, "Theory of one and two donors in silicon," *J. Phys. Condens. Matter* **27**, 154208 (2015).
- N. Cassidy, P. Blenkinsopp, I. Brown, R. J. Curry, B. N. Murdin, R. Webb, and D. Cox, "Single ion implantation of bismuth," *Phys. Status Solidi Appl. Mater. Sci.* **218**, 2000237 (2021).
- G. W. Morley, P. Lueders, M. Hamed Mohammady, S. J. Balian, G. Aeppli, C. W. Kay, W. M. Witzel, G. Jeschke, and T. S. Monteiro, "Quantum control of hybrid nuclear-electronic qubits," *Nat. Mater.* **12**, 103–107 (2013).
- T. Peach, K. Homewood, M. Lourenco, M. Hughes, K. Saedi, N. Stavrias, J. Li, S. Chick, B. Murdin, and S. Clowes, "The effect of lattice damage and annealing conditions on the hyperfine structure of ion implanted bismuth donors in silicon," *Adv. Quantum Technol.* **1**, 1800038 (2018).
- A. Chatterjee, P. Stevenson, S. de Franceschi, A. Morello, N. P. de Leon, and F. Kuemmeth, "Semiconductor qubits in practice," *Nat. Rev. Phys.* **3**, 157–177 (2021).
- A. D. Becke, "Density-functional exchange-energy approximation with correct asymptotic behavior," *Phys. Rev. A* **38**, 3098–3100 (1988).
- C. Lee, E. Yang, and R. G. Parr, "Development of the Colle-Salvetti correlation-energy formula into a functional of the electron density," *Phys. Rev. B* **37**, 785–789 (1988).
- M. J. Frisch, G. W. Trucks, H. B. Schlegel, G. E. Scuseria, M. A. Robb, J. R. Cheeseman, G. Scalmani, V. Barone, G. A. Petersson, H. Nakatsuji, X. Li, M. Caricato, A. V. Marenich, J. Bloino, B. G. Janesko, R. Gomperts, B. Mennucci, H. P. Hratchian, J. V. Ortiz, A. F. Izmaylov, J. L. Sonnenberg, D. Williams-Young, F. Ding, F. Lipparini, F. Egidi, J. Goings, B. Peng, A. Petrone, T. Henderson, D. Ranasinghe, V. G. Zakrzewski, J. Gao, N. Rega, G. Zheng, W. Liang, M. Hada, M. Ehara, K. Toyota, R. Fukuda, J. Hasegawa, M. Ishida, T. Nakajima, Y. Honda, O. Kitao, H. Nakai, T. Vreven, K. Throssell, J. A. Montgomery, Jr., J. E. Peralta, F. Ogliaro, M. J. Bearpark, J. J. Heyd, E. N. Brothers, K. N. Kudin, V. N. Staroverov, T. A. Keith, R. Kobayashi, J. Normand, K. Raghavachari, A. P. Rendell, J. C. Burant, S. S. Iyengar, J. Tomasi, M. Cossi, J. M. Millam, M. Klene, C. Adamo, R. Cammi, J. W. Ochterski, R. L. Martin, K. Morokuma, O. Farkas, J. B. Foresman, and D. J. Fox, Gaussian, Inc., Wallingford, CT, 2016.
- J. J. Boland, "Manipulating chlorine atom bonding on the Si(100)- (2×1) surface with the STM," *Science* **262**, 1703–1706 (1993).
- H. P. Noh, "Adsorption of Bi on Si(001) surface: An atomic view," *J. Vac. Sci. Technol. B* **12**, 2097 (1994).
- S. Y. Bulavenko, I. F. Koval, P. V. Melnik, N. G. Nakhodkin, and H. J. Zandvliet, "STM investigation of the initial adsorption stage of Bi on Si(100)- (2×1) and Ge(1 0 0)- (2×1) surfaces," *Surf. Sci.* **482–485**, 370–375 (2001).
- S. Tang and A. J. Freeman, "Bi-induced reconstructions on Si(100)," *Phys. Rev. B* **50**, 1701–1704 (1994).
- Y. Qian, M. J. Bedzyk, P. F. Lyman, T. L. Lee, S. Tang, and A. Freeman, "Structure and surface kinetics of bismuth adsorption on Si(001)," *Phys. Rev. B - Condens. Matter Mater. Phys.* **54**, 4424–4427 (1996).
- C. J. Kirkham, V. Brázdová, and D. R. Bowler, "Bi on the Si(001) surface," *Phys. Rev. B* **86**, 035328 (2012).
- G. E. Franklin, S. Tang, J. C. Woicik, M. J. Bedzyk, A. J. Freeman, and J. A. Golovchenko, "High-resolution structural study of Bi on Si(001)," *Phys. Rev. B* **52**, R5515–R5519 (1995).
- O. Warschkow, N. J. Curson, S. R. Schofield, N. A. Marks, H. F. Wilson, M. W. Radny, P. V. Smith, T. C. G. Reusch, D. R. McKenzie, and M. Y. Simmons, "Reaction paths of phosphine dissociation on silicon (001)," *J. Chem. Phys.* **144**, 014705 (2016).
- Q. Gao, C. C. Cheng, P. J. Chen, and W. J. Choyke, "Comparison of Cl_2 and HCl adsorption on Si(100)- (2×1) ," *Thin Solid Films* **225**, 140–144 (1993).
- T. V. Pavlova, E. S. Skorokhodov, G. M. Zhidomirov, and K. N. Eltsov, "Ab Initio study of the early stage of Si epitaxy on the chlorinated Si(100) surface," *J. Phys. Chem. C* **123**, 19806–19811 (2019).
- A. Farzaneh and R. E. Butera, "Si epitaxy on Cl-Si(100)," *Appl. Surf. Sci.* **589**, 152877 (2022).
- J. H. Owen, Q. Campbell, R. Santini, J. A. Ivie, A. D. Baczewski, S. W. Schmucker, E. Bussmann, S. Misra, and J. N. Randall, "Al-alkyls as acceptor dopant precursors for atomic-scale devices," *J. Phys. Condens. Matter* **33**, 464001 (2021).
- G. Scappucci, G. Capellini, B. Johnston, W. M. Klesse, J. A. Miwa, and M. Y. Simmons, "A complete fabrication route for atomic-scale, donor-based devices in single-crystal germanium," *Nano Lett.* **11**, 2272–2279 (2011).
- E. V. Hofmann, T. J. Stock, O. Warschkow, R. Conybeare, N. J. Curson, and S. R. Schofield, "Room temperature incorporation of arsenic atoms into the germanium (001) surface," *Angew. Chem. - Int. Ed.* **62**, e202213982 (2023).